Made available by Hasselt University Library in https://documentserver.uhasselt.be

Redox-Responsive Nanocapsules for the Spatiotemporal Release of Miltefosine in Lysosome: Protection against Leishmania

Peer-reviewed author version

Tiwari, Rajeshwari; Banerjee, Saswati; Tyde, Deepak; Das Saha, Krishna; ETHIRAJAN, Anitha; Mukherjee, Niladri; Chattopadhy, Samit; PRAMANIK, Sumit & Das, Amitava (2021) Redox-Responsive Nanocapsules for the Spatiotemporal Release of Miltefosine in Lysosome: Protection against Leishmania. In: BIOCONJUGATE CHEMISTRY, 32 (2) , p. 245 -253.

DOI: 10.1021/acs.bioconjchem.0c00667
Handle: http://hdl.handle.net/1942/33881

Redox-Responsive Nanocapsules for the Spatiotemporal Release of Miltefosine in Lysosome: Protection against *Leishmania*

Rajeswari Tiwari[a, b]‡, Saswati Banerjee[c]‡, Deepak Tyde[a,b], Krishna Das Saha [c], Anitha Ethirajan[d], Niladri Mukherjee [c]*, Samit Chattopadhy[e] *, Sumit Kumar Pramanik[a, b] * and Amitava Das[f]*

[a] CSIR-Central Salt & Marine Chemicals Research Institute, G.B. Marg, Bhavnagar: 364002, Gujarat, India

[b] Academy of Scientific and Innovative Research (AcSIR), Ghaziabad, Uttar Pradesh-201 002, India

[c] Cancer Biology and Inflammatory Disorder Division, CSIR-Indian Institute of Chemical Biology, 4 Raja S. C. Mullick Road, Kolkata-700032, India

[d] Institute for Materials Research (IMO), Hasselt University, Wetenschapspark 1, 3590 Diepenbeek, Belgium

[e] BITS Pilani, K K Birla Goa Campus, Goa 403726, India.

[f] Indian Institute of Science Education and Research Kolkata; Mohanpur: 741246, West Bengal, India.

ABSTRACT: Leishmaniasis, a vector-borne disease is caused by intracellular parasite *leishmania donovani*. Unlike most intracellular pathogens, *leishmania donovani* are lodged in parasitophorous vacuoles and replicate within the phagolysosomes in macrophages. Effective vaccines against this disease are still under development, while the efficacy of the available drugs is being questioned owing to the toxicity for nonspecific distribution in human physiology and the reported drug-resistance developed by *leishmania donovani*. Thus, a stimuli-responsive nanocarrier that allows specific localization and release of the drug in the lysosome has been highly sought after for addressing two crucial issues, lower drug toxicity and a higher drug efficacy. We report here a unique lysosome targeting polymeric nanocapsules, formed via inverse mini-emulsion technique, for stimuli-responsive release of the drug miltefosine in the lysosome of macrophage RAW 264.7 cell line. A benign polymeric backbone, with a disulfide bonding susceptible to an oxidative cleavage, is utilized for the organelle-specific release of miltefosine. Oxidative rapture of the disulfide bond is induced by intracellular glutathione (GSH) as an endogenous stimulus. Such a stimuli-responsive release of the drug miltefosine in the lysosome of macrophage RAW 264.7 cell line over a few hours helped in achieving an improved drug efficacy by 200-times as compared to pure miltefosine. Such a drug formulation could attribute to a new line of treatment for leishmaniasis.

More than 20 species of *leishmania* cause symptomatic leishmaniasis are responsible for a range of clinical manifestations varying from cutaneous ulcerations to fatal visceral infections. The most common one among all these variations is the visceral leishmaniasis, or kala-azar, is a vector-borne disease and the majority of parasites reside in macrophages of mammalian cells.[1-3] Visceral leishmaniasis generally turns lethal if untreated. Despite its epidemiological importance, [4-5] leishmaniasis is classified by WHO as the so-called neglected disease that has failed to attract adequate financial support as well as the support of the academic bodies along with the public-health authorities for prevention and control the disease.[6-7] A recent survey report published by Cloots et. al reveals that the majority (~95%) of the visceral leishmaniasis in 2017 occurred in just ten countries, including Bangladesh, India, and Nepal.[8] According to a recent WHO report, visceral leishmaniasis elimination has resulted in a substantial decrease (~ 85%) in the caseload in the Indian subcontinent. Implementation of the elimination strategy primarily relied on effective case management and disease surveillance, as well as integrated vector control and availability of efficient clinical interventions. However, studies have also established that asymptomatic infection has outnumbered incident of visceral leishmaniasis by a factor of nine in the Indian subcontinent and presumably, this reduction in visceral leishmaniasis cases may not be the true reflection of the decrease in disease transmission.[9-10] Affected areas constitute foci of anthroponotic transmission of the parasite and this enhances the possibility of the fast-spreading of drug-resistant parasites. Despite its acute need and advancements in clinical insights, effective vaccine against leishmaniasis is still under development. Effective treatment primarily relies on the chemotherapeutic drugs, like antimonials (sodium stibogluconate and meglumine antimoniate), paromomycin, oral miltefosine and a liposomal formulation of amphotericin B.[11-13] Such prevalent chemotherapy is far from satisfactory and development of acquired resistance to these drugs has made clinical prognosis and treatment even more challenging.[14-15] Further, recent clinical data have also shown that the efficacy of the same drug and dosing regimen differs for different geographical locations. Literature reports also confirm that *leishmania* promastigotes enter the dermal macrophages by utilizing the host CR3 and this prevents the circulating phagocytes and nonimmune serum to kill the parasites.[16-18] This adds to the challenge for the treatment of leishmaniasis.[17-18] To get around this problem, suitably functionalized nanocarrier with encapsulated antileishmanial drugs could be a promising approach for treating leishmaniasis. Appropriate surface functionalization of the nanocarriers could help in overcoming the biological barrier and uptake in macrophages. This helps in releasing the drug at the targeted site and

lead to a much higher local concentration as well as therapeutic efficiency.[4-5, 19-21] Use of such suitably functionalized polymeric nanocarriers has been increasingly used for targeted drug release and improving its therapeutic efficacy.[22-25] Polymeric nanocarriers with core-shell nanocapsule morphology could carry, store, and release one or a combination of drugs, reporter molecules for clinical diagnostics or biochemical processes.[26-28] Additionally, the chemical versatility of polymers provides an option for post-functionalization of the outer surface of the nanocapsules, which play an essential role in the interactions with their surroundings.[26, 29] Furthermore, the stimuli-responsive shell of nanocapsules serves as a smart barrier, which protects the encapsulated payloads from the surrounding environment and releases payloads in a pulsatile or selective way.[30-31]

There are a few literature reports on GSH-responsive nanocarriers that undergo an efficient GSH-induced rapture of the polymeric backbone for programmed site-specific endogenous payload release. However, the majority of such examples are based on self-assembled macrocycle and such nanocapsules typically suffer from the undesired nonspecific leaching loss of the encapsulated payload.[32-34] A target-specific, as well as stimuli-responsive nanocapsule could be more appropriate for precision therapeutic for preclinical studies.[29, 35] In our recent reports, we have demonstrated that the appropriate choice of the polymeric backbone along with surface functionalization of the polymeric nanocapsules lead to an organelle-specific release of the payload.[29] There are only a few literature reports that have exploited such a methodology.[36]

It has been recently shown that after internalization in the host cells, *L. donovani* parasitophorous vacuoles are efficiently fused with lysosomes and hijack host cell lysosomes involved in plasma membrane repair to induce invasion in fibroblasts.[37-38] *L. donovani* modulates the endo-lysosomal pathway to reside in a modified early endocytic compartment and inhibits lysosomal transport in macrophages.[39] These results indicate the possibility of selective delivery of an anti-leishmanial drug to lysosome could be useful for developing future therapeutic intervention. Miltefosine, the only approved oral drug for treating visceral and cutaneous leishmaniasis, is the outcome of the major therapeutic advancement for clinical management of leishmaniasis.[40-41] Considering these, we designed a redox-responsive polymeric shell with a relatively higher loading capacity of antileishmanial drug, miltefosine. To the best of our knowledge, this is the first report on primary amines-acid anhydride reaction chemistry for the synthesis of fully biodegradable polymeric nanocarriers (MNCs). Presumably, the presence of acid functionalities onto the surface of the nanocapsules helped us to maintain the appropriate lipophilicity for specific localization at the lysosome of the Raw 264.7 cells.[42-43] This MNC was found to be non-toxic and effectively internalized in the Raw 264.7 cells. Lysosome specificity and the rapture of the disulfide bond resulted in the release of miltefosine in the lysosome. This helped in achieving an improvement of the drug efficacy by 200 times.

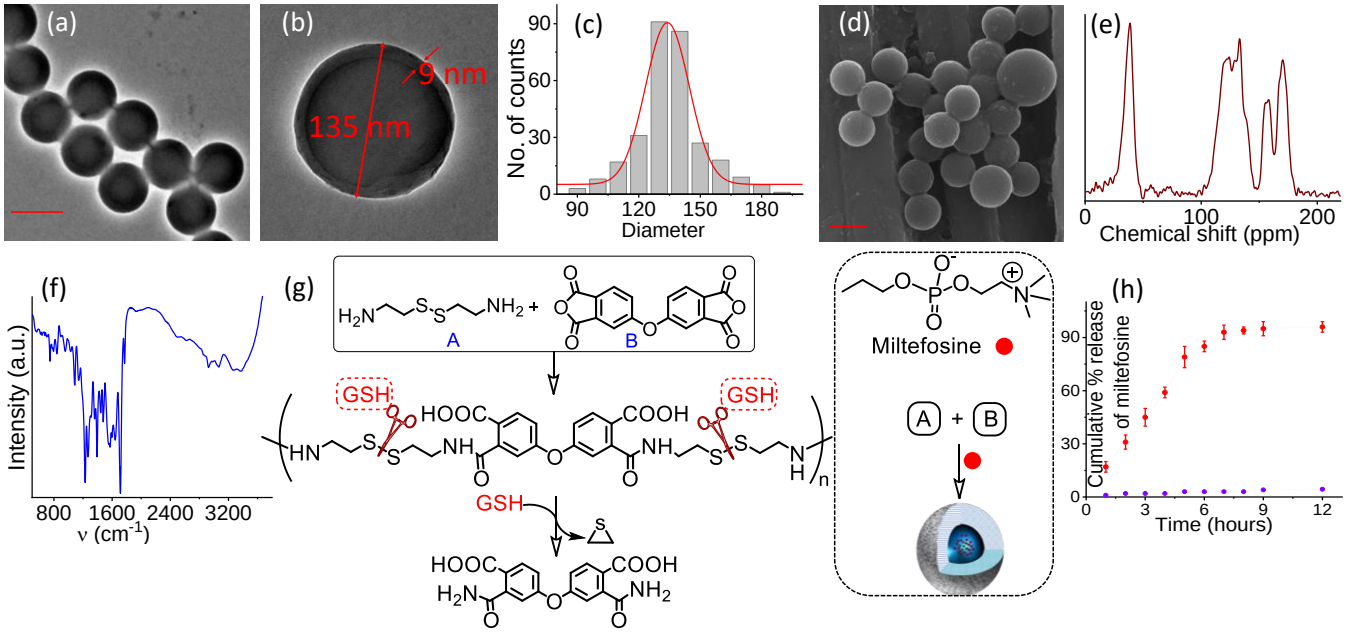

Figure 1. (a) TEM image of the nanocapsules, (b) enlarge image of a single nanocapsule with 9 nm wall thickness, (c) size distribution of the nanocapsules, (d) SEM images of the nanocapsules, (e) CPMAS NMR spectrum of nanocapsules, (f) FT-IR spectra of the nanocapsules, (g) schematic representation for the synthesis and GSH-induced degradation of the polymeric backbone of the capsule shell by GSH, and (h) the GSH-mediated cumulative percentage release of miltefosine at lysosomal pH (pH 5.0). Representative plots of disulfide-linked nanocapsules (red color) versus non-disulfide-linked nanocapsules (violet) versus time on glutathione treatment, indicating that the in situ generated GSH (induced by glutathione enzyme) induced rapture of the polymeric backbone of the capsule shell and release of the encapsulated miltefosine. Scale bar 200 nm.

The redox responsive nanocapsules were synthesized by interfacial inverse mini-emulsion reaction.[44] The synthesis process is shown schematically in Figure S1. The reaction between –NH2 groups from cystamine and anhydride groups from 4,4′-oxydiphthalic anhydride in a stoichiometric ratio occurred at the water-in-oil droplet interface to form a cross-linked polymeric shell. The drug miltefosine was used as an encapsulated payload for studying the anti-leishmanial activity. The reaction between two bifunctional monomers was performed at room temperature in the presence of triethylamine as a base catalyst for the

nanocapsule formation. The detailed synthesis procedure is given in supporting information. Briefly, cyclohexane was used as the continuous phase and the dispersed phase employed consists of cystamine, 2,2-bis(aminomethyl)propane-1,3-diamine, dimethoxy-sulphoxide, miltefosine and sodium chloride solution. A sodium chloride solution was used to build up the osmotic pressure of droplets in the continuous hydrophobic phase and rhodamine/miltefosine was encapsulated in the hydrophilic core. After pre-emulsification, entire dispersion was subjected to probe sonication to obtain the stable nanodroplets of the dispersed phase. Subsequently, an additive phase containing the base catalyst and the 4,4′-oxydiphthalic anhydride monomer in cyclohexane was slowly introduced into the continuous phase and then the reaction mixture was stirred for 6 hours to ensure the completion of the polymerization reaction for the generation of the nanocapsules having miltefosine trapped inside the core.

The resulting nanocapsules were thoroughly characterized by dynamic light scattering (DLS), scanning electron microscopy (SEM), and transmission electron microscopy (TEM). The reaction efficiency was studied thermogravimetically in the form of the solid content of the obtained dispersion. As the drug is hydrophilic, the effective encapsulation efficiency of MNCs in the aqueous phase (after redispersion)was calculated by a previously reported protocol and found to be about 95 %.[29] Chemical analyses of the insoluble product was performed using high-resolution solid-state 13C nuclear magnetic resonance (CPMS) and Fourier-transform infrared (FTIR) spectroscopy. SEM and TEM images indicated that nanocapsules had a spherical morphology with a mean diameter of 130 ± 10 nm with a narrower size distribution (Figures 1a-d). The close examination of these nanocapsules under TEM (Figure 1b) revealed a hollow interior with a thin shell (~12.0 ± 4 nm thick), which agreed well with the results of previous reports.[44] The DLS results suggested a mean size of 160 nm with a polydispersity index of ~ 0.07 and this was consistent with TEM/SEM results. The surface potential was evaluated and zeta potential of −23.7 ± 3 mV was obtained.

Formation of the amide-bond formation through the amine–anhydride reaction was confirmed from the ^{13}C NMR spectra recorded for the product. In Figure 1e, the NMR data obtained for the air-dried nanocapsule sample is depicted. The aliphatic carbons are observed in the range between 25 - 49 ppm. The ^{13}C signals ranging from 110 ppm - 150 ppm originate from the aromatic ring of the 4,4′-oxydiphthalic anhydride, which is used for polymerization. The peak at 164 ppm is attributed to the $C{=}O_{Amide}$ functionality. A well-defined intense signal at 181 ppm confirms the formation of -COOH group. Results of the FT-IR (Figure 1f) spectrum further corroborate this structure elucidation. The typical bands at 1635 cm−1 and 1525 cm−1 are assigned to the stretching and bending vibrations, respectively, for the $C{=}O_{Amide}$ and $N{-}H_{Amide}$ of the amide linkage. The band at 3500 cm-1 originates from the $N{-}H_{Amide}$ vibration as well as the stretching vibration of the $–OH_{COOH}$.

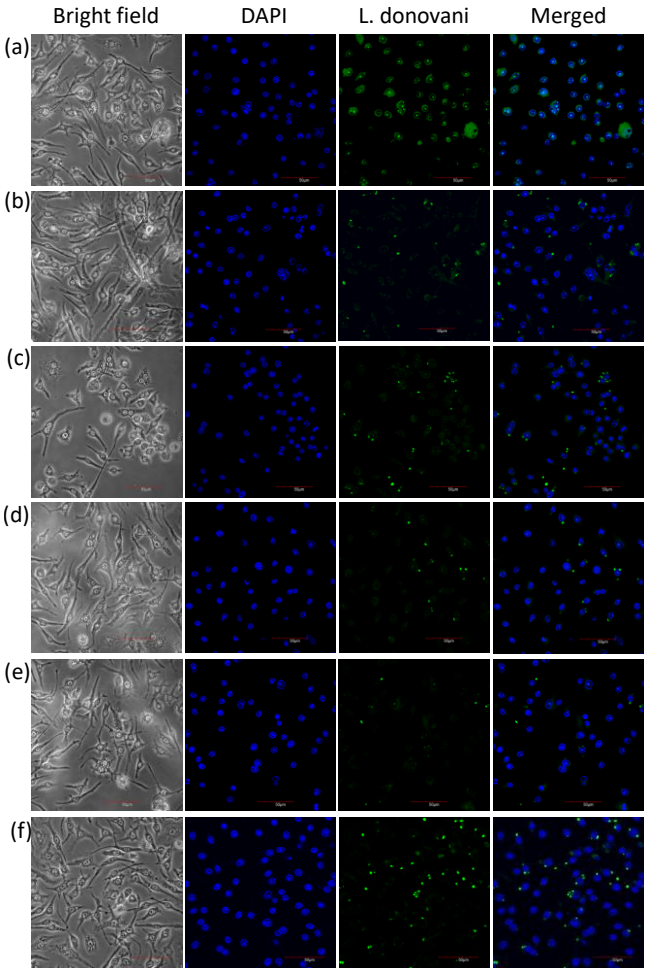

Figure 2. Confocal microscopic images of intracellular CFSE stained *L. donovani* inhibition after 24h of MNCs treatment at different concentrations: (a) infected macrophages, infected macrophages incubated with (b) 8 ng/mL MNCs (c) 20 ng/mL MNCs (d) 40 ng/mL MNCs (e) 100 ng/mL MNCs (f) 100 ng/mL miltefosine. Magnification used 120X. Scale bar 50 µM.

Choice of the set of monomer that was used for the reaction helped us in having disulfide linkages in the polymeric backbone. To initially examine the redox-responsiveness of these disulfide bonds of the polymeric nanocapsules, MNCs were first incubated with GSH at lysosomal pH (pH 5.0). And the payload release profile of MNCs for the dispersion incubated with GSH was monitored by HPLC. Under lysosomal pH conditions, a release of ~96% miltefosine was observed in 8h. Another control experiment using nanocapsule without disulfide

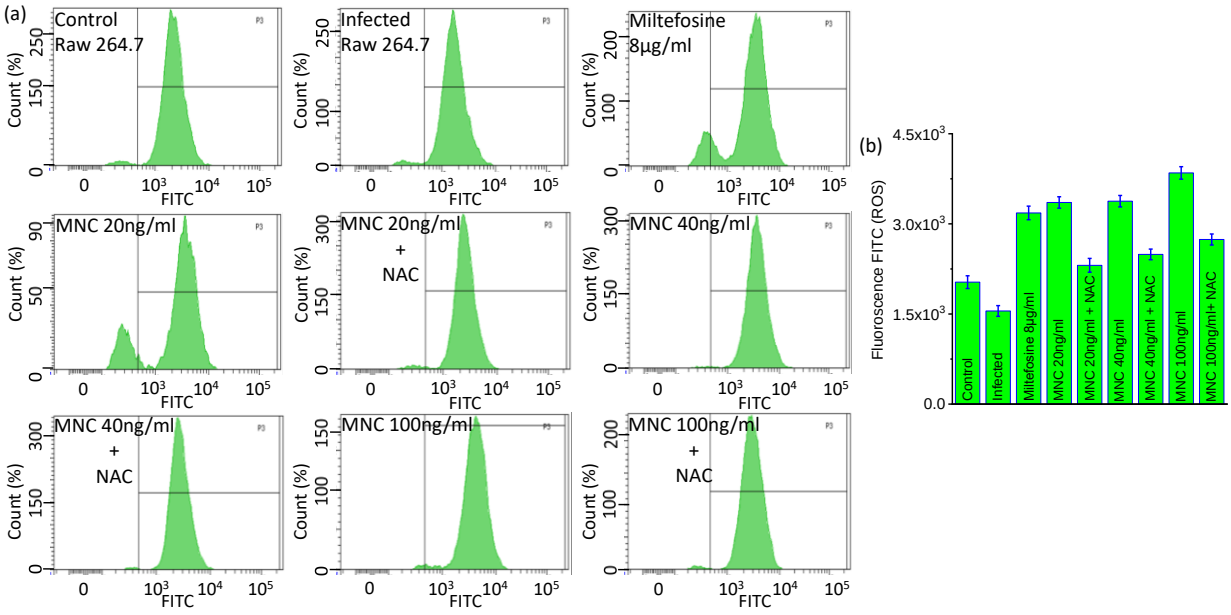

Figure 3. Effect of ROS on miltefosine and MNCs treatment: Estimation of ROS generation in control, infected and treated (MNCs and miltefosine) macrophage Raw 264.7 cell line. NAC was used as a ROS inhibitor. (a) changes in the amplitude of fluorescence of FITC-histogram of DCFDA exposed macrophage Raw 264.7 cell line. (b) bar diagram of median fluorescence index values of DCFDA, proportional with the ROS generation. All values are expressed as mean ± SEM from triplicate assays from three independent experiments (P values ≤ 0.05 (*) or ≤ 0.01 (**) vs. infected panel).

linkages in the polymeric backbone showed insignificant release of miltefosine (Figure 1g-h), confirming the efficacy of the GSH-induced redox process in cleaving the disulfide bonds with subsequent release of the payload. The release of the drug for 8 hrs also ensured the crucial issue of sustained-release—a typical factor for better efficacy of any drug.

The biocompatibility of nanocapsules and MNCs was evaluated using MTT assays on macrophage Raw 264.7 (derived from BALB/c mouse liver) cell lines upon incubation for up to 24h. Typically nanocapsules and MNCs (up to 40 µg/mL) showed negligible toxicity against RAW 264.7 cell line, suggesting an excellent biocompatibility profile (Figure S2a).

The leishmanicidal activity tests were performed in vitro with intracellular *L. donovani* parasites. The macrophage Raw 264.7 cell line was infected with promastigotes of *L. donovani* (Strain AG83) at a ratio of 1:10 and the effect of MNCs on the survival of *L. donovani* amastigotes was evaluated after 24 hrs of treatment. MNCs was found to be highly efficient in killing the cell internalized *L. donovani* in respect to the positive control of pure miltefosine. LC_{50} value found for MNCs and miltefosine was 67 ± 2 ng/mL and 3 ± 0.11 µg/mL respectively (Figure S2b-c), indicates the higher efficacy of nano formulated miltefosine against *L. donovani* amastigotes as compared with the normal dose of the same drug.

For quantitative assessment of intracellular leishmanicidal activity of MNCs, Raw 264.7 cell line was infected with carboxyfluorescein N-succinimidyl ester (CFSE)-labelled parasites, monitored by FACS as well as confocal microscopy. The infected Raw 264.7 cells were treated with MNCs (20, 40, and 100 ng/mL) and pure miltefosine (8 µg/mL) was used as a positive control. FACS results demonstrated the dose-dependent depletion of parasite count signified by the decrease of fluorescence intensity as well as the reduction in the infected Raw 264.7 cells count (Figure S3). The resulting confocal micrographs (monitored at 480/30 nm) also depicted the reduction in green fluorescence emitting parasite count in the MNCs treated panels (Figure 2). The decrease in fluorescence intensity signified the increase in recovery from *L. donovani* parasitemia. The confocal microscopy results together with the flow cytometry data unambiguously confirmed the higher efficacy of nanoformulated miltefosine against intracellular *L. donovani* as compared with miltefosine alone.

Reactive oxygen (ROS) and nitrogen (RNS) species-mediated apoptosis-like cell death, induced by miltefosine, in *leishmania* infected cells is widely accepted as one of the most accepted mechanistic pathway associated with the antileishmanial activity of miltefosine.[45] To encounter host defence, *leishmania* parasites implement strategies to overcome the stress induced by the oxidative environment and preserve redox homeostasis.[45] Two important molecules that are vital in controlling *leishmania* are superoxide anion (O_2^-) and nitric oxide (NO).[46] At the early phase of infection by *leishmania*, O_2^- is produced as part of the oxidative burst of macrophages in response to phagocytosis.[47] Whereas the second oxidant produced by macrophages is NO, which, in contrast to O_2^-, is generated after activation of macrophages by Interferon-gamma and tumour necrosis factor. The importance of oxidative burst, triggered by miltefosine in intracellular *L. donovani* removal, is well appreciated and accepted.[48] The ROS generation in control and *leishmania* co-cultured macrophage Raw 264.7 cell line was

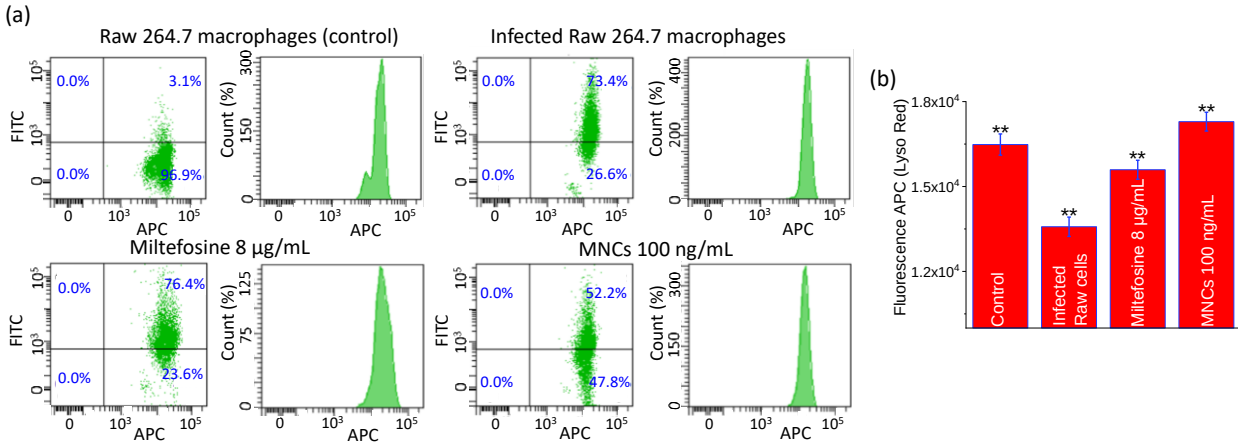

Figure 4. (a) Quantitative evaluation of phagolysosomal maturation during the anti-leishmanial activity of MNCs by using flow cytometry: Lysotracker red is used as marker for lysosomal maturation. The four quadrants denote different subpopulations of exposed Raw 264.7 macrophages, i.e. Q1 (CFSE-tagged *L. donovani*), Q2 (Lysotracker red and CFSE-tagged *L. donovani* expressing), Q3 (Double negative, not expressing any of the Lysotracker red and CFSE-tagged *L. donovani*), Q4 (Lysotracker red expressing cells). (b) Bar diagram of median fluorescence index values of LysoTracker Red. Infected Raw 264.7 macrophages denoted compromised lysosome maturation which was increased in the treated panels'per their anti-leishmanial activity. All values are expressed as mean ± SEM from triplicate assays from three independent experiments (P values ≤ 0.05 (*) or ≤ 0.01 (**) vs. infected panel).

estimated by staining with 2′,7′-dichlorofluorescin diacetate (DCFDA). Cellular ROS oxidizes non-emissive DCFDA to a strongly fluorescence dye 2',7' –dichlorofluorescein (DCF, λ_{Ems} ~ 529nm; λ_{Ems} = 0.96 in Water/ 10 mM PBS, fluorescein was used as reference) and this fluorescence ON response is directly proportional to the amount of the formation of DCF.[49] ROS level in *L. donovani* infected cells was significantly lower than untreated controls (P<0.001) (Figure 3). Subsequent to miltefosine (8µg/mL) and MNCs (20, 40, 100 ng/mL) exposure, macrophages infected with *L. donovani* showed a significant increase (≥2-fold, P<0.01) in ROS levels (Figure 3). The pre-treatment of cells with the glutathione precursor with N-acetyl cysteine (NAC; an efficient ROC scavenger) successfully inhibited the miltefosine induced ROS level. The miltefosine induced ROS generation pattern for the present study is comparable to values reported in the literature.[45]

It has been argued that the NO (produced in situ) in miltefosine treated *L. donovani* infected macrophages attributes to the effectiveness of miltefosine for anti-microbicidal activity. The NO metabolism was assessed by FACS using a fluorescence dye 4,5-Diaminofluorescein diacetate (DAF-2DA). Low basal levels of NO were detected in the cell-free culture supernatants of *L. donovani* infected macrophages, correlating with the progression of the disease. Two-fold higher NO levels were found in infected macrophages treated with a higher dose of MNCs (100 ±0.41 ng/mL; P<0.001µM) as compared to infected control and the response was dose-dependent (20, 40, 100 ng/mL; P<0.001; Figure S4), harmonizing with the previous reports.[50] The pre-treatment of infected cells with N-monomethyl-L-arginine (L-NMMA), an efficient NO inhibitor, significantly down-regulated miltefosine controlled NO production (Figure S4). Thus, these results indicate that the in vitro leishmanicidal effect of MNCs occurred via an increase in production of NO without adverse effects on macrophages.[51]

Since the MNCs shows better efficacy than that of miltefosine alone, the possibility that the MNCs manipulate the phagolysomal machinery of macrophages to restrict *leishmania* growth.[52] A phagolysosome, is a cytoplasmic body formed by the fusion of a phagosome with a lysosome in a process that occurs during phagocytosis. *L. donovani* parasites reside inside the macrophages and delays phagosome maturation.[53] Phagosome maturation causes a severe drop in lumen pH that significantly alters the biochemical nature of phagosome lumen that ultimately destroy pathogens.[54] The intracellular pathogens modulate the phagosomal maturation at the very early stage, either by avoiding the fusion of the pathogen containing phagosomes with lysosomes or by escaping from phagosomes to replicate in the cytosol.[55] Therefore, the improved performance of MNCs in intracellular anti-leishmanial activity can be revealed by monitoring the dynamics of fusion of phagosome with the lysosome. The phagolysosomal maturation is broadly divided into four stages; (i) early phagosome stage having the molecular marker Rab-5, (ii) phagolysosomal fusion stage with molecular marker V-H+ ATPase, (iii) late phagosome stage characterized by molecular markers Cathepsin-D, Rab-7 and (iv) endosome recycling stage with molecular marker Rab-9 (Figure S5).[55-56]

The attenuated phagolysosomal maturation in *L. donovani*-infected macrophages may lead to an impaired acquisition of parasitic features. Concomitant with phagosome maturation is the progressive acidification of the phagosome lumen, which aids the killing and digestion of intracellular *L. donovani* in the lysosome.[57]

The study of the dynamics of lysosomal vesicle during MNCs treatment is important for evaluating the efficiency of MNCs and comparing that with pure miltefosine to ascertain its improved performance in an intracellular anti-leishmanial activity. LysoTracker was utilized during flow cytometry and confocal microscopy for estimating the lysosomal incorporation during *L. donovani* infection and MNCs treatment. The flow cytometry and the confocal microscopic analysis of macrophages depicted

the dose-dependent clearance of the intracellular parasites (intracellular parasites are inversely proportional with the number of lysosomal vesicles) (Figure 4 and Figure 5).

The sequential propagation of phagolysosomal maturation has been verified with visualization of Rab-5, V-H+ ATPase, Cathepsin-D, Rab-7, and Rab-9. The Rab-family GTPases are known to mediate the progression between the early, late, and lysosome fusion stages. Specifically, Rab5 is a characteristic marker of the early phagosome that drives the transition to the late phagosome stage, which is defined by the presence of Rab7.[58] Low basal levels of Rab-5 expression was observed in *L. donovani* infected macrophages. The expression of RAB5 was profoundly higher in MNC treated infected macrophages, which is an essential and rate-limiting component for early endosome fusion (Figure 6).

This fusion of phagosome with lysosome is the crucial step for intracellular removal of the *L. donovani* through phagolysosomal maturation,[59] can be monitored by quantitative and qualitative evaluation of V-H+ ATPase.[60] A significant increase of V-H+ ATPase marker has been observed for both miltefosine and MNCs treated infected macrophages (≥2 fold, $P<0.01$). Among these, the increment of V-H+ ATPase marker is slightly more for MNCs than that of miltefosine alone (Figure S6). The confocal microscopy images depicted the upregulation of Rab-7 and Cathepsin-D marker for the MNCs treated panels, supports the phagolysosomal maturation and parasite elimination in a dose-dependent manner (Figure 5 and 6). The expression of Rab-9, a characteristic marker of late phagosomes and phagolysosomes,[61] was also significantly upregulated at 4 h following MNC treatment (Figure 6), indicates reduced parasitic load. Altogether, these results suggest the MNCs initiate and regulate the phagolysosome maturation mechanism in controlling the parasitic load in *L. donovani* infected macrophages.

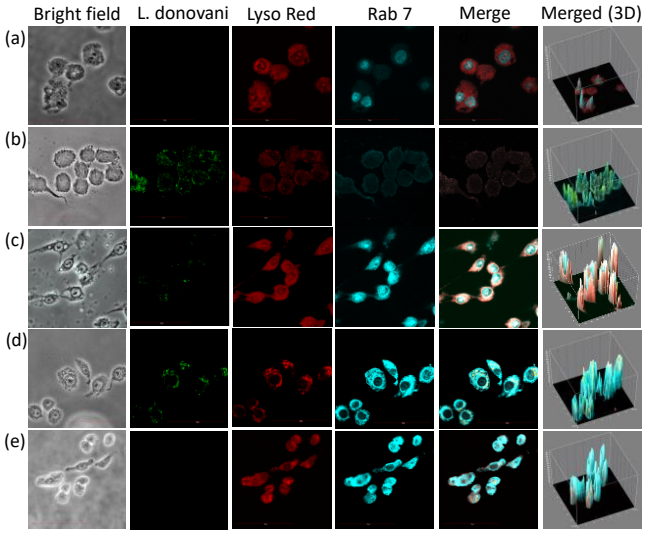

Figure 5. Confocal microscope images of lysosomal Maturation in *L. donovani* infected Raw 264.7 macrophages (incubated with Rab-7 antibodies and Lysotracker-Red): Raw 264.7 macrophages were infected with *L. donovani* at a ratio of 1:10 for 4 hrs, washed and treated with MNCs for 24 hrs. (a)Raw 264.7 macrophages (b) Raw 264.7 macrophages infected with *L. donovani* (c) miltefosine 8 µg/mL, as positive control (d) 20 ng/mL MNCs (e) 40 ng/mL MNCs. Scale bar 10 µm.

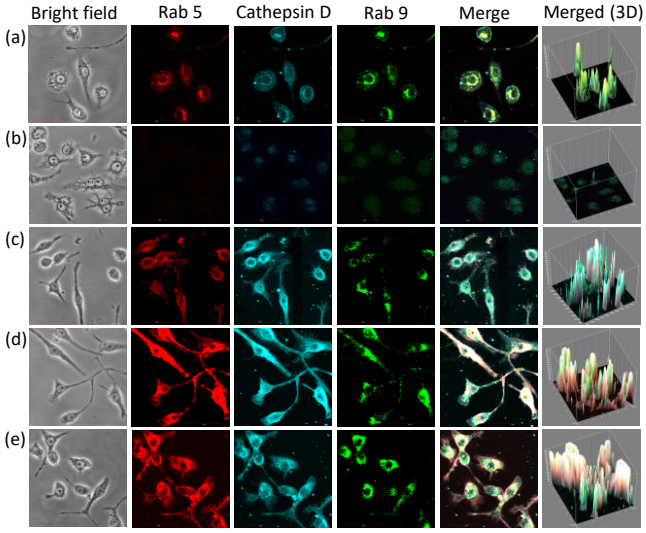

Figure 6. Confocal microscope images of lysosomal Maturation in *L. donovani* infected Raw 264.7 macrophages (incubated with Rab-5, Cathepsin-D and Rab-9 markers): Raw 264.7 macrophages were infected with *L. donovani* at a ratio of 1:10 for 4 hrs, washed and treated with MNCs for 24 hrs. (a) Raw 264.7 macrophages (b) Raw 264.7 macrophages infected with *L. donovani* (c) miltefosine 8 µg/mL, as positive control (d) 20 ng/mL MNCs (e) 40 ng/mL MNCs. Scale bar 10 µm.

Miltefosine is the only approved oral drug for treating visceral and cutaneous leishmaniasis. However, miltefosine resistance, or rather drug non-susceptibility, is reported for *L. donovani* promastigote clones owing to a defect in drug internalization into the parasite and increased drug efflux from the parasite is believed to be the most plausible mechanism that attributes to this resistance. To get around this problem, we have designed a lysosome-specific polymeric nanocarrier that allows a stimuli-responsive release of the drug miltefosine. The polymeric backbone of the physiologically benign nanocarrier is susceptible to a certain redox environment and participates in a stimuli-responsive reductive rapture (induced by GSH) for the lysosome-specific release of the drug miltefosine. This also helped in improving the drug efficacy by 200 times and lowering the drug-induced cell mortality when compared with the identical dosage of pure miltefosine. The design aspect and the results achieved could help in successfully demonstrating the scope for developing new drug formulations for treating critical diseases with lesser deleterious secondary effect(s) that occurs in addition to the desired therapeutic effect of a drug or medication. This work is also expected to stimulate further interest and investigations of organelle-specific, as well as stimuli-responsive nanocapsules for various biomedical applications, including theranostics.

ASSOCIATED CONTENT

Supporting Information.
The Supporting Information is available free of charge at https://pubs.acs.org/doi/10.1021/XXXXXX.

AUTHOR INFORMATION

Corresponding Author

Niladri Mukherjee; Email- niladrizoology@gmail.com
Samit Chattopadhy; Email- samitc@goa.bits-pilani.ac.in
Amitava Das; Email- a.das@csmri.res.in

Sumit Kumar Pramanik; Email- sumitpramanik@csmcri.res.in.

Author Contributions

‡These authors contributed equally.

Notes

The authors declare no competing financial interest.

ACKNOWLEDGEMENT

A. Das acknowledges SERB (India) Grants (SB/S1/IC-23/2013& JCB/2017/000004) and DBT Grant (BT/PR22251/NNT/28/1274/2017) for supporting this research. N. Mukherjee acknowledges SERB (India) Grant PDF/2016/001437 and K. Das acknowledges the grant EMR/2015/001674 for supporting this research. Financial support from SERB (DST/INSPIRE/03/2017/002477) is acknowledged by R.T.

REFERENCES

1. Georgiadou, S. P.; Makaritsis, K. P.; Dalekos, G. N., Leishmaniasis revisited: Current aspects on epidemiology, diagnosis and treatment. *J Transl Int Med* **2015,** *3* (2), 43-50.
2. Iqbal, H.; Ishfaq, M.; Wahab, A.; Abbas, M. N.; Ahmad, I.; Rehman, A.; Zakir, M., Therapeutic modalities to combat leishmaniasis, a review. *Asian Pacific Journal of Tropical Disease* **2016,** *6* (1), 1-5.
3. Torres-Guerrero, E.; Quintanilla-Cedillo, M. R.; Ruiz-Esmenjaud, J.; Arenas, R., Leishmaniasis: a review. *F1000Res* **2017,** *6*, 750-750.
4. Nagle, A. S.; Khare, S.; Kumar, A. B.; Supek, F.; Buchynskyy, A.; Mathison, C. J. N.; Chennamaneni, N. K.; Pendem, N.; Buckner, F. S.; Gelb, M. H.; Molteni, V., Recent Developments in Drug Discovery for Leishmaniasis and Human African Trypanosomiasis. *Chemical Reviews* **2014,** *114* (22), 11305-11347.
5. Gutiérrez, V.; Seabra, A. B.; Reguera, R. M.; Khandare, J.; Calderón, M., New approaches from nanomedicine for treating leishmaniasis. *Chemical Society Reviews* **2016,** *45* (1), 152-168.
6. Varma, D. M.; Redding, E. A.; Bachelder, E. M.; Ainslie, K. M., Nano- and Microformulations to Advance Therapies for Visceral Leishmaniasis. *ACS Biomaterials Science & Engineering* **2020**.
7. Khatami, A.; Firooz, A.; Gorouhi, F.; Khamesiour, A.; Dowlati, Y., Cutaneous leishmaniasis. *The Lancet Infectious Diseases* **2008,** *8* (8), 458.
8. Cloots, K.; Uranw, S.; Ostyn, B.; Bhattarai, N. R.; Le Rutte, E.; Khanal, B.; Picado, A.; Chappuis, F.; Hasker, E.; Karki, P.; Rijal, S.; Boelaert, M., Impact of the visceral leishmaniasis elimination initiative on Leishmania donovani transmission in Nepal: a 10-year repeat survey. *The Lancet Global Health* **2020,** *8* (2), e237-e243.
9. Picado, A.; Singh, S. P.; Rijal, S.; Sundar, S.; Ostyn, B.; Chappuis, F.; Uranw, S.; Gidwani, K.; Khanal, B.; Rai, M.; Paudel, I. S.; Das, M. L.; Kumar, R.; Srivastava, P.; Dujardin, J. C.; Vanlerberghe, V.; Andersen, E. W.; Davies, C. R.; Boelaert, M., Longlasting insecticidal nets for prevention of Leishmania donovani infection in India and Nepal: paired cluster randomised trial. *BMJ* **2010,** *341*, c6760.
10. Rijal, S.; Uranw, S.; Chappuis, F.; Picado, A.; Khanal, B.; Paudel, I. S.; Andersen, E. W.; Meheus, F.; Ostyn, B.; Das, M. L.; Davies, C.; Boelaert, M., Epidemiology of Leishmania donovani infection in high-transmission foci in Nepal. *Tropical medicine & international health : TM & IH* **2010,** *15 Suppl 2*, 21-8.
11. Faral-Tello, P.; Greif, G.; Satragno, D.; Basmadjián, Y.; Robello, C., Leishmania infantum isolates exhibit high infectivity and reduced susceptibility to amphotericin B. *RSC Medicinal Chemistry* **2020,** *11* (8), 913-918.
12. Ahmed, H.; Curtis, C. R.; Tur-Gracia, S.; Olatunji, T. O.; Carter, K. C.; Williams, R. A. M., Drug combinations as effective anti-leishmanials against drug resistant Leishmania mexicana. *RSC Medicinal Chemistry* **2020,** *11* (8), 905-912.
13. Corpas-Lopez, V.; Moniz, S.; Thomas, M.; Wall, R. J.; Torrie, L. S.; Zander-Dinse, D.; Tinti, M.; Brand, S.; Stojanovski, L.; Manthri, S.; Hallyburton, I.; Zuccotto, F.; Wyatt, P. G.; De Rycker, M.; Horn, D.; Ferguson, M. A. J.; Clos, J.; Read, K. D.; Fairlamb, A. H.; Gilbert, I. H.; Wyllie, S., Pharmacological Validation of N-Myristoyltransferase as a Drug Target in Leishmania donovani. *ACS Infectious Diseases* **2019,** *5* (1), 111-122.
14. Pérez-Victoria, F. J.; Sánchez-Cañete, M. P.; Seifert, K.; Croft, S. L.; Sundar, S.; Castanys, S.; Gamarro, F., Mechanisms of experimental resistance of Leishmania to miltefosine: Implications for clinical use. *Drug Resistance Updates* **2006,** *9* (1), 26-39.
15. Croft, S. L.; Sundar, S.; Fairlamb, A. H., Drug resistance in leishmaniasis. *Clin Microbiol Rev* **2006,** *19* (1), 111-26.
16. de Carvalho, R. V. H.; Lima-Junior, D. S.; da Silva, M. V. G.; Dilucca, M.; Rodrigues, T. S.; Horta, C. V.; Silva, A. L. N.; da Silva, P. F.; Frantz, F. G.; Lorenzon, L. B.; Souza, M. M.; Almeida, F.; Cantanhêde, L. M.; Ferreira, R. d. G. M.; Cruz, A. K.; Zamboni, D. S., Leishmania RNA virus exacerbates Leishmaniasis by subverting innate immunity via TLR3-mediated NLRP3 inflammasome inhibition. *Nature Communications* **2019,** *10* (1), 5273.
17. Priyanka, P.; Vandana, P.; Medha, J., Nanocarriers for Effective Topical Delivery of Anti-Infectives. *Current Nanoscience* **2012,** *8* (4), 491-503.
18. Walker, D. M.; Oghumu, S.; Gupta, G.; McGwire, B. S.; Drew, M. E.; Satoskar, A. R., Mechanisms of cellular invasion by intracellular parasites. *Cellular and molecular life sciences : CMLS* **2014,** *71* (7), 1245-63.
19. Singh, H.; Tiwari, K.; Tiwari, R.; Pramanik, S. K.; Das, A., Small Molecule as Fluorescent Probes for Monitoring Intracellular Enzymatic Transformations. *Chemical Reviews* **2019,** *119* (22), 11718-11760.
20. Singh, H.; Sreedharan, S.; Oyarzabal, E.; Mahapatra, T. S.; Green, N.; Shih, Y.-Y. I.; Das, M.; Thomas, J. A.; Pramanik, S. K.; Das, A., Mitochondriotropic lanthanide nanorods: implications for multimodal imaging. *Chemical Communications* **2020,** *56* (57), 7945-7948.
21. Tiwari, R.; Shinde, P. S.; Sreedharan, S.; Dey, A. K.; Vallis, K.; Mhaske, S. B.; Pramanik, S. K.; Das, A., Photoactivable Prodrug for Simultaneous Release of Mertansine, and CO along with a BODIPY Derivative as a Luminescent Marker in Mitochondria: A Proof of Concept for NIR Image-Guided Cancer Therapy. *Chemical Science* **2021**.
22. Singh, A. P.; Biswas, A.; Shukla, A.; Maiti, P., Targeted therapy in chronic diseases using nanomaterial-based drug delivery vehicles. *Signal Transduction and Targeted Therapy* **2019,** *4* (1), 33.
23. Rosenblum, D.; Joshi, N.; Tao, W.; Karp, J. M.; Peer, D., Progress and challenges towards targeted delivery of cancer therapeutics. *Nature Communications* **2018,** *9* (1), 1410.
24. Awino, J. K.; Gudipati, S.; Hartmann, A. K.; Santiana, J. J.; Cairns-Gibson, D. F.; Gomez, N.; Rouge, J. L., Nucleic Acid Nanocapsules for Enzyme-Triggered Drug Release. *Journal of the American Chemical Society* **2017,** *139* (18), 6278-6281.
25. Fu, S.; Zhang, Y.; Guan, S.; Huang, Q.; Wang, R.; Tian, R.; Zang, M.; Qiao, S.; Zhang, X.; Liu, S.; Fan, X.; Li, X.; Luo, Q.; Hou, C.; Xu, J.; Dong, Z.; Liu, J., Reductive-Responsive, Single-Molecular-Layer Polymer Nanocapsules Prepared by Lateral-Functionalized Pillar[5]arenes for Targeting Anticancer Drug Delivery. *ACS Applied Materials & Interfaces* **2018,** *10* (17), 14281-14286.
26. Veetil, A. T.; Chakraborty, K.; Xiao, K.; Minter, M. R.; Sisodia, S. S.; Krishnan, Y., Cell-targetable DNA nanocapsules for spatiotemporal release of caged bioactive small molecules. *Nature Nanotechnology* **2017,** *12* (12), 1183-1189.
27. Pramanik, S. K.; Seneca, S.; Peters, M.; D'Olieslaeger, L.; Reekmans, G.; Vanderzande, D.; Adriaensens, P.; Ethirajan, A., Morphology-dependent pH-responsive release of hydrophilic payloads using biodegradable nanocarriers. *RSC Advances* **2018,** *8* (64), 36869-36878.
28. Seneca, S.; Pramanik, S. K.; D'Olieslaeger, L.; Reekmans, G.; Vanderzande, D.; Adriaensens, P.; Ethirajan, A., Nanocapsules with stimuli-responsive moieties for controlled release employing light and enzymatic triggers. *Materials Chemistry Frontiers* **2020,** *4* (7), 2103-2112.
29. Pramanik, S. K.; Sreedharan, S.; Singh, H.; Khan, M.; Tiwari, K.; Shiras, A.; Smythe, C.; Thomas, J. A.; Das, A., Mitochondria Targeting Non-Isocyanate-Based Polyurethane Nanocapsules for Enzyme-Triggered Drug Release. *Bioconjugate Chemistry* **2018,** *29* (11), 3532-3543.
30. Tan, C.; Arshadi, M.; Lee, M. C.; Godec, M.; Azizi, M.; Yan, B.; Eskandarloo, H.; Deisenroth, T. W.; Darji, R. H.; Pho, T. V.; Abbaspourrad, A., A Robust Aqueous Core–Shell–Shell Coconut-like Nanostructure for Stimuli-Responsive Delivery of Hydrophilic Cargo. *ACS Nano* **2019,** *13* (8), 9016-9027.
31. Pramanik, S. K.; Pal, U.; Choudhary, P.; Singh, H.; Reiter, R. J.; Ethirajan, A.; Swarnakar, S.; Das, A., Stimuli-Responsive Nanocapsules for the Spatiotemporal Release of Melatonin: Protection against Gastric Inflammation. *ACS Applied Bio Materials* **2019,** *2* (12), 5218-5226.
32. Ling, X.; Tu, J.; Wang, J.; Shajii, A.; Kong, N.; Feng, C.; Zhang, Y.; Yu, M.; Xie, T.; Bharwani, Z.; Aljaeid, B. M.; Shi, B.; Tao, W.; Farokhzad, O. C., Glutathione-Responsive Prodrug Nanoparticles for Effective Drug Delivery and Cancer Therapy. *ACS Nano* **2019,** *13* (1), 357-370.
33. Yin, W.; Ke, W.; Lu, N.; Wang, Y.; Japir, A. A.-W. M. M.; Mohammed, F.; Wang, Y.; Pan, Y.; Ge, Z., Glutathione and Reactive Oxygen Species

Dual-Responsive Block Copolymer Prodrugs for Boosting Tumor Site-Specific Drug Release and Enhanced Antitumor Efficacy. *Biomacromolecules* **2020,** *21* (2), 921-929.
34. Sreedharan, S.; Tiwari, R.; Tyde, D.; Aderinto, S. O.; Pramanik, S. K.; Das, A.; Thomas, J. A., Nanocarriers used as probes for super-resolution microscopy. *Materials Chemistry Frontiers* **2021**.
35. Kumar Pramanik, S.; Losada-Pérez, P.; Reekmans, G.; Carleer, R.; D'Olieslaeger, M.; Vanderzande, D.; Adriaensens, P.; Ethirajan, A., Physicochemical characterizations of functional hybrid liposomal nanocarriers formed using photo-sensitive lipids. *Scientific Reports* **2017,** *7* (1), 46257.
36. Deng, S.; Gigliobianco, M. R.; Censi, R.; Di Martino, P., Polymeric Nanocapsules as Nanotechnological Alternative for Drug Delivery System: Current Status, Challenges and Opportunities. *Nanomaterials* **2020,** *10* (5), 847.
37. Forestier, C. L.; Machu, C.; Loussert, C.; Pescher, P.; Späth, G. F., Imaging host cell-Leishmania interaction dynamics implicates parasite motility, lysosome recruitment, and host cell wounding in the infection process. *Cell host & microbe* **2011,** *9* (4), 319-30.
38. Cavalcante-Costa, V. S.; Costa-Reginaldo, M.; Queiroz-Oliveira, T.; Oliveira, A. C. S.; Couto, N. F.; dos Anjos, D. O.; Lima-Santos, J.; Andrade, L. O.; Horta, M. F.; Castro-Gomes, T., Leishmania amazonensis hijacks host cell lysosomes involved in plasma membrane repair to induce invasion in fibroblasts. *Journal of Cell Science* **2019,** *132* (6), jcs226183.
39. Verma, J. K.; Rastogi, R.; Mukhopadhyay, A., Leishmania donovani resides in modified early endosomes by upregulating Rab5a expression via the downregulation of miR-494. *PLOS Pathogens* **2017,** *13* (6), e1006459.
40. Sunyoto, T.; Potet, J.; Boelaert, M., Why miltefosine-a life-saving drug for leishmaniasis-is unavailable to people who need it the most. *BMJ global health* **2018,** *3* (3), e000709.
41. Dorlo, T. P. C.; Balasegaram, M.; Beijnen, J. H.; de Vries, P. J., Miltefosine: a review of its pharmacology and therapeutic efficacy in the treatment of leishmaniasis. *Journal of Antimicrobial Chemotherapy* **2012,** *67* (11), 2576-2597.
42. Yu, H.; Xiao, Y.; Jin, L., A Lysosome-Targetable and Two-Photon Fluorescent Probe for Monitoring Endogenous and Exogenous Nitric Oxide in Living Cells. *Journal of the American Chemical Society* **2012,** *134* (42), 17486-17489.
43. Singh, H.; Sreedharan, S.; Tiwari, K.; Green, N. H.; Smythe, C.; Pramanik, S. K.; Thomas, J. A.; Das, A., Two photon excitable graphene quantum dots for structured illumination microscopy and imaging applications: lysosome specificity and tissue-dependent imaging. *Chemical Communications* **2019,** *55* (4), 521-524.
44. Kuypers, S.; Pramanik, S. K.; D'Olieslaeger, L.; Reekmans, G.; Peters, M.; D'Haen, J.; Vanderzande, D.; Junkers, T.; Adriaensens, P.; Ethirajan, A., Interfacial thiol–isocyanate reactions for functional nanocarriers: a facile route towards tunable morphologies and hydrophilic payload encapsulation. *Chemical Communications* **2015,** *51* (87), 15858-15861.
45. Deep, D. K.; Singh, R.; Bhandari, V.; Verma, A.; Sharma, V.; Wajid, S.; Sundar, S.; Ramesh, V.; Dujardin, J. C.; Salotra, P., Increased miltefosine tolerance in clinical isolates of Leishmania donovani is associated with reduced drug accumulation, increased infectivity and resistance to oxidative stress. *PLOS Neglected Tropical Diseases* **2017,** *11* (6), e0005641.
46. Carneiro, P. P.; Conceição, J.; Macedo, M.; Magalhães, V.; Carvalho, E. M.; Bacellar, O., The Role of Nitric Oxide and Reactive Oxygen Species in the Killing of Leishmania braziliensis by Monocytes from Patients with Cutaneous Leishmaniasis. *PLOS ONE* **2016,** *11* (2), e0148084.
47. Carneiro, P. P.; Conceição, J.; Macedo, M.; Magalhães, V.; Carvalho, E. M.; Bacellar, O., The Role of Nitric Oxide and Reactive Oxygen Species in the Killing of Leishmania braziliensis by Monocytes from Patients with Cutaneous Leishmaniasis. *PloS one* **2016,** *11* (2), e0148084-e0148084.
48. Deep, D. K.; Singh, R.; Bhandari, V.; Verma, A.; Sharma, V.; Wajid, S.; Sundar, S.; Ramesh, V.; Dujardin, J. C.; Salotra, P., Increased miltefosine tolerance in clinical isolates of Leishmania donovani is associated with reduced drug accumulation, increased infectivity and resistance to oxidative stress. *PLoS neglected tropical diseases* **2017,** *11* (6), e0005641-e0005641.
49. Zhang, X.-F.; Zhang, J.; Liu, L., Fluorescence Properties of Twenty Fluorescein Derivatives: Lifetime, Quantum Yield, Absorption and Emission Spectra. *Journal of Fluorescence* **2014,** *24* (3), 819-826.
50. Islamuddin, M.; Chouhan, G.; Want, M. Y.; Ozbak, H. A.; Hemeg, H. A.; Afrin, F., Immunotherapeutic Potential of Eugenol Emulsion in Experimental Visceral Leishmaniasis. *PLOS Neglected Tropical Diseases* **2016,** *10* (10), e0005011.
51. Olivier, M.; Gregory, D. J.; Forget, G., Subversion mechanisms by which Leishmania parasites can escape the host immune response: a signaling point of view. *Clin Microbiol Rev* **2005,** *18* (2), 293-305.
52. Visser, J. G.; Van Staden, A. D. P.; Smith, C., Harnessing Macrophages for Controlled-Release Drug Delivery: Lessons From Microbes. *Frontiers in Pharmacology* **2019,** *10* (22).
53. Erwig, L.-P.; McPhilips, K. A.; Wynes, M. W.; Ivetic, A.; Ridley, A. J.; Henson, P. M., Differential regulation of phagosome maturation in macrophages and dendritic cells mediated by Rho GTPases and ezrin–radixin–moesin (ERM) proteins. *Proceedings of the National Academy of Sciences* **2006,** *103* (34), 12825.
54. Canton, J.; Khezri, R.; Glogauer, M.; Grinstein, S., Contrasting phagosome pH regulation and maturation in human M1 and M2 macrophages. *Mol Biol Cell* **2014,** *25* (21), 3330-3341.
55. Pauwels, A. M.; Trost, M.; Beyaert, R.; Hoffmann, E., Patterns, Receptors, and Signals: Regulation of Phagosome Maturation. *Trends Immunol* **2017,** *38* (6), 407-422.
56. Rocha, M. I.; Dias, F.; Resende, M.; Sousa, M.; Duarte, M.; Tomás, A. M.; Castro, H., Leishmania infantum Enhances Migration of Macrophages via a Phosphoinositide 3-Kinase γ-Dependent Pathway. *ACS Infectious Diseases* **2020,** *6* (7), 1643-1649.
57. Jubrail, J.; Morris, P.; Bewley, M. A.; Stoneham, S.; Johnston, S. A.; Foster, S. J.; Peden, A. A.; Read, R. C.; Marriott, H. M.; Dockrell, D. H., Inability to sustain intraphagolysosomal killing of Staphylococcus aureus predisposes to bacterial persistence in macrophages. *Cellular Microbiology* **2016,** *18* (1), 80-96.
58. Harrison, R. E.; Bucci, C.; Vieira, O. V.; Schroer, T. A.; Grinstein, S., Phagosomes fuse with late endosomes and/or lysosomes by extension of membrane protrusions along microtubules: role of Rab7 and RILP. *Molecular and cellular biology* **2003,** *23* (18), 6494-506.
59. Settembre, C.; Di Malta, C.; Polito, V. A.; Arencibia, M. G.; Vetrini, F.; Erdin, S.; Erdin, S. U.; Huynh, T.; Medina, D.; Colella, P.; Sardiello, M.; Rubinsztein, D. C.; Ballabio, A., TFEB Links Autophagy to Lysosomal Biogenesis. *Science* **2011,** *332* (6036), 1429-1433.
60. Settembre, C.; Zoncu, R.; Medina, D. L.; Vetrini, F.; Erdin, S.; Erdin, S.; Huynh, T.; Ferron, M.; Karsenty, G.; Vellard, M. C.; Facchinetti, V.; Sabatini, D. M.; Ballabio, A., A lysosome-to-nucleus signalling mechanism senses and regulates the lysosome via mTOR and TFEB. *EMBO J* **2012,** *31* (5), 1095-1108.
61. Flannagan, R. S.; Heit, B.; Heinrichs, D. E., Intracellular replication of Staphylococcus aureus in mature phagolysosomes in macrophages precedes host cell death, and bacterial escape and dissemination. *Cellular Microbiology* **2016,** *18* (4), 514-535.

Insert Table of Contents artwork here

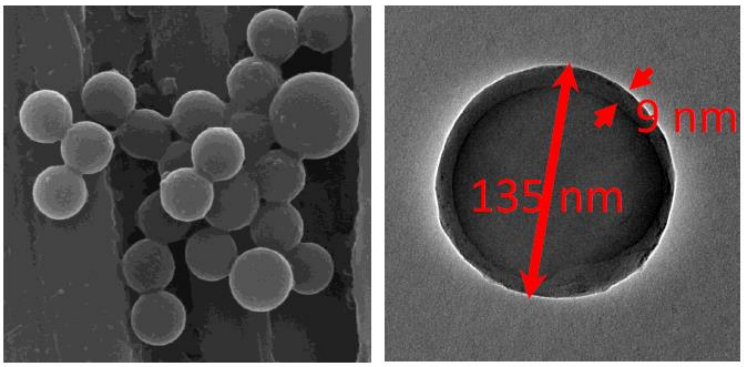
9 nm
135 nm

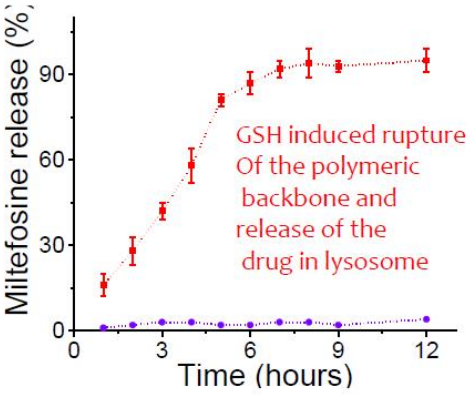
Miltefosine release (%)
0
30
60
90
0
3
6
9
12
Time (hours)
GSH induced rupture
Of the polymeric
backbone and
release of the
drug in lysosome

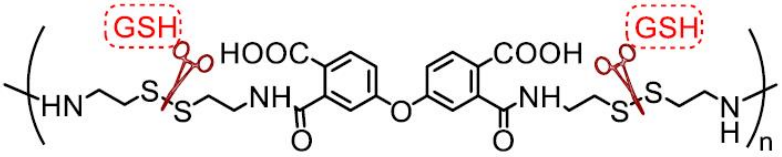
GSH
HOOC
COOH
GSH
HN
S
S
NH
O
O
NH
S
S
N
H
n

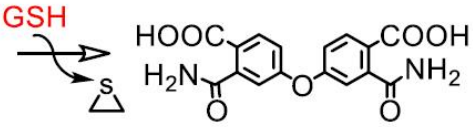
GSH
HOOC
COOH
H2N
NH2
O
O
O
S